# Nylon 6 Induced Morphological Developments and Electrical Conductivity Improvements of Polypropylene/Carbon Black Composites

**Guangshun Chen,[1] Bo Yang,[1,2] Shaoyun Guo[1]**

[1]*State Key Laboratory of Polymer Materials Engineering, Polymer Research Institute of Sichuan University, Chengdu, Sichuan, China 610065*
[2]*Research Center of Laser Fusion, China Academy of Engineering Physics, Mianyang, China 621900*

Received 11 December 2008; accepted 27 April 2009
DOI 10.1002/app.30684
Published online 24 June 2009 in Wiley InterScience (www.interscience.wiley.com).

**ABSTRACT:** In this study, a polar conductive filler [carbon black (CB)], a nonpolar polymer [polypropylene (PP)], and a polar polymer [nylon 6 (PA6)] were chosen to fabricate electrically conductive polymer composites by melt blending and compression molding. The morphological developments of these composites were studied. Scanning electron microscopy results showed that in a CB-filled PP/PA6 (CPA) composite, CB particles were selectively dispersed in PA6 phases and could make the dispersed particles exist as microfiber particles, which could greatly improve the electrical conductivity. The PA6 and CB contents both could affect the morphologies of these composites. The results of electrical resistivity measurements of these composites proved the formation of conductive networks. The resistivity–temperature behaviors of these composites were also studied. For CB-filled PP (CP) composites, there were apparent positive temperature coefficient (PTC) and negative temperature coefficient (NTC) effects and an unrepeatable resistivity–temperature characteristic. However, for CPA composites, there were no PTC or NTC effects from room temperature to 180°C, and the resistivity–temperature behavior showed a repeatable characteristic; this proved that CB particles were selectively dispersed in the PA6 phase from another point of view. All experimental results indicated that the addition of PA6 to a CP composite could lead to an expected morphological structure and improve the electrical conductivity of the CP composite. © 2009 Wiley Periodicals, Inc. J Appl Polym Sci 114: 1848–1855, 2009

**Key words:** composites; morphology; nylon; poly(propylene) (PP)

## INTRODUCTION

In general, the incorporation of electrically conductive fillers decreases the mechanical properties and processability of polymers. Nevertheless, to fulfill electrical conductivity requirements of filler-filled conductive polymer composites, the content of conductive fillers must be higher than the critical content or percolation threshold. Therefore, the crucial aspect for solving this contrast is lowering the percolation threshold of the conductive filler. Much effort has been expended to prepare electrically conductive composites with a low electrical percolation threshold. Many reports have focused on the modification of the distribution of a conductive filler in a polymer matrix. For example, Yoon et al.[1] reported that the electrical conductivity of carbon black (CB)/polymer composites is tremendously influenced by the amine-terminated coupling treatment of CB because of its action as an assister of electrical conduction. Grunlan et al.[2] and Hu et al.[3] found that mixing CB and polymer suspensions or emulsions under high-speed stirring could lead to a low percolation threshold because of conductive pathway formation during the drying of the latex. Tjong et al.[4] and Hu et al.[5] reduced the percolation threshold of polypropylene (PP)/multiwalled nanotube and poly(ethylene terephthalate)/multiwalled nanotube nanocomposites by high-shear-rate processing and coagulation, respectively. Garmabi and Naficy[6] reported that a PP/nylon 6 (PA6)/CB composite with a three-dimensional microfibrillar conducting network could be prepared *in situ* with a melt-spinning process, and the percolation threshold of the system could be reduced when the aspect ratio of the conducting phase was increased by the development of a microfibrillar morphology. Nogales et al.,[7] Zou et al.,[8] and Lu et al.[9] reported that the percolation threshold

*Correspondence to:* S. Guo (nic7702@scu.edu.cn).
Contract grant sponsor: Special Funds for Major State Basic Research Projects of China; contract grant number: 2005CB623800.
Contract grant sponsor: National Natural Science Foundation of China; contract grant number: 50603016.
Contract grant sponsor: Program for Changjiang Scholars and Innovative Research Team in University.

could be reduced by *in situ* polycondensation or/and polymerization. Polymer composites produced from particle composite systems can also have a low percolation threshold.[10] Some studies have reported that the filler aspect ratio and arrangement strongly affect the electrical behaviors of some conductive composites.[11–13] In addition, Al-Saleh and Sundararaj[14] reported that in CB–PP/polystyrene (PS) blends, CB preferentially localized in the PS phase. Upon the introduction of a styrene–butadiene–styrene (SBS) triblock copolymer, CB showed higher affinity to the polybutadiene (PBD) section of the SBS copolymer, which was selectively localized at the interface between PP and PS. There was a 40% reduction in the percolation threshold in a 70/30 PP/PS blend upon the addition of 5 vol % SBS because of the selective localization of CB in the PBD phase and the change in the blend morphology; this indicated that it is possible to obtain a low percolation threshold by the design of a special morphological structure for conductive composites.

In fact, it is well known that for immiscible polymer blends, different morphological structures can be developed during blend processing, and the morphological development in the melt state is controlled by the interaction of domain deformation, breakup, and coalescence. The flow field deforms domains and, if sufficiently strong, breaks them into smaller domains. At the same time, the flow field provides for collisions between domains, which may cause their coalescence. The interfacial tension between two polymers provides a thermodynamic driving force for resisting domain deformation and encouraging coalescence. The morphological development is controlled by the competition of the flow forces that deform and break domains and the forces that oppose deformation and breakup. This limit typically depends on the rheological characteristics of the components, such as the viscosity ratio and first normal stress differences.[15–17] According to this idea, it is possible to design a kind of morphological structure with double continuous phases in polymer blends by the selection of a suitable polymer blending system and good control of the processing parameters by which the dispersed phase particles can overlap one another. If we let the conductive fillers disperse into the overlapped oriented dispersed phase, a three-dimensional conductive network can be easily formed with a lower conductive filler content.

In filler-filled polymer composites with two different kinds of polymers, the competitive adsorption of polymer melts on a solid filler surface is determined by the filler–polymer interaction. When solid filler particles are mixed with a polymer blend consisting of polymers A and B, the location of the filler should be predicted by Young's equation:[18]

$$\omega = \frac{(\gamma_{\text{filler}-A} - \gamma_{\text{filler}-B})}{\gamma_{A-B}} \quad (1)$$

where $\omega$ is called the wetting coefficient, $\gamma_{\text{filler}-A}$, $\gamma_{\text{filler}-B}$, and $\gamma_{A-B}$ are the interfacial energies between polymer A and the filler, between polymer B and the filler, and between the polymers, respectively. Filler particles are expected to be selectively located in one of two polymer phases in which the polymer has a higher interaction with the filler surface: at $\omega > 0$, that is, $\gamma_{\text{filler}-A} > \gamma_{\text{filler}-B}$, filler particles are in polymer B or at the interface, and at $\omega < 0$, that is, $\gamma_{\text{filler}-A} < \gamma_{\text{filler}-B}$, filler particles are in polymer A or at the interface. Wu et al.[19] calculated the interfacial energy between PP and CB ($\gamma_{\text{PP–CB}}$) to be 19.8 mJ/m$^2$ and the interfacial energy between PA6 and CB ($\gamma_{\text{PA6–CB}}$) to be 17.1 mJ/m$^2$ on the basis of the results in ref. 20. Obviously, in PP/PA6/CB composites, CB particles are expected to be selectively located in the PA6 phase.

As described previously, it is possible to design a favorable morphological structure for a CB-filled PP/PA6 composite in which there are two kinds of networks, a dispersed phase network and an electrically conductive filler network in the dispersed phase. Therefore, a good electrically conductive network can be obtained at a lower filler concentration on the whole, and there will be a lower percolation threshold for this composite. Garmabi and Naficy[6] prepared a PP/PA6/CB composite *in situ* using a melt-spinning process to obtain a three-dimensional microfibrillar conducting network, but it is also worth investigating how the addition of PA6 to CB-filled PP (CP) composites affects the morphology structure, the dispersion of CB, the electrical conductivity, and the resistivity–temperature characteristic by a simple melt-mixing process. In this study, a nonpolar polymer (PP), a polar polymer (PA6), and a polar conductive filler (CB) were chosen to prepare an electrically conductive composite with this kind of morphological structure. Meanwhile, it is well acknowledged that the volume expansion of the polymeric matrix in its melting range will cause electrical paths or networks to be broken, and this will result in positive temperature coefficient (PTC) effects. If CB particles are veritably selected in PA6, there is a comparatively low expansion ratio for PA6 from room temperature to the melting point of PP (180°C); this indicates that at this temperature range, there will be no PTC effects for the composite made of PP, PA6, and CB, so the experimental results of PTC effects can be used to verify our foregoing assumption from another point of view.

## EXPERIMENTAL

### Materials

The PP used was T30S (supplied by Dushanzi Petrochemical Co. of Petrochina Co., Ltd., Dushanzi,

**TABLE I**
**Property Indices of CB**

| Item | Unit | Index |
|---|---|---|
| Special surface area | $m^2/g$ | 660 |
| Dibutyl phthalate adsorption | $10^{-5}$ $m^3/kg$ | 260 |
| Tint strength | % | 90 |
| Heat loss | % | 2.0 |
| Apparent density | $kg/m^3$ | 180 |
| pH | — | 8.0–9.0 |

**TABLE II**
**Sample Codes for Different CB-Filled Composites**

| Sample | | $m_{PP}$ | $m_{PA}$ | $\varphi_{CB}$ (vol %) |
|---|---|---|---|---|
| CP | CP-1 | 100 | 0 | 2.5 |
| | CP-2 | 100 | 0 | 5.0 |
| CPA | CPA1 | 90 | 10 | 2.5 |
| | CPA2-1 | 80 | 20 | 2.5 |
| | CPA2-2 | 80 | 20 | 5.0 |
| | CPA3 | 70 | 30 | 2.5 |
| | CPA4 | 60 | 40 | 2.5 |

Xinjiang, China) with a melt flow index of 3.6 g/10 min. The PA6 used was M23400 (supplied by Guangdong Xinhui Meida Nylon Co., Ltd., Jiangmen, Guangdong, China) with a melt flow index of 1.82 g/10 min. The conductive CB was E900 (supplied by Sichuan Zhenghao Special Carbon Technology, Ltd., Chengdu, Sichuan, China); the property indices are listed in Table I.

### Sample preparation

PA6 was dried in a drying oven at 105°C for at least 10 h before being used. Sample codes for the different CB-filled composites are listed in Table II ($\varphi_{CB}$ is the volume content of CB in the composites). The desired amounts of CB, PP, and PA were mixed in an internal mixer (Rheocord 90, Hakke, Karlsruhe, Germany) for 10 min at 190°C and 30 rpm (only with the PP matrix) or at 230°C and 40 rpm (both with PP and PA6 matrices), and then the mixtures were compression-molded into samples 1 mm thick at 190 or 240°C, respectively; the copper meshes were also compression-molded on both sides of these samples as electrodes for resistivity measurements.

### Measurements and characterization

The samples with volume resistance lower than $10^3$ Ω were measured by the four-point probe method. When the volume resistance was higher than $10^3$ Ω, a ZC46A high-resistance electrometer and a ZC36 electrode (Shanghai Precision & Scientific Instrument Co., Ltd., Shanghai, China) were used. The sample geometries were $1 \times 10 \times 10$ and $1 \times 80 \times 80$ $mm^3$ for the four-point probe and high-resistance meter, respectively. The $1 \times 10 \times 80$ $mm^3$ samples were used in resistivity–temperature behavior testing, for which a WCY-SJ temperature programming control system (Nanjing Sangli Electronic Equipment Works, Nanjing, China) was used; the heating medium was silicone oil, the samples were immersed in it to avoid oxidation, and the testing temperature ranged from room temperature to 180°C at a heating rate of 2°C/min. When the temperature reached 180°C, it was kept there for 5 min, and then the sample was cooled to room temperature. The resistivity–temperature behaviors were recorded during each heating process. The volume resistances were measured with a YD9820A programming insulation resistance tester (Changzhou Yangzi Electronic Co., Ltd., Changzhou, China). The phase structures of all composites were observed by scanning electron microscopy (SEM) analysis. Before observation, the samples were brittle-fractured under the temperature of liquid nitrogen, and the fractured surfaces were coated with a silver–

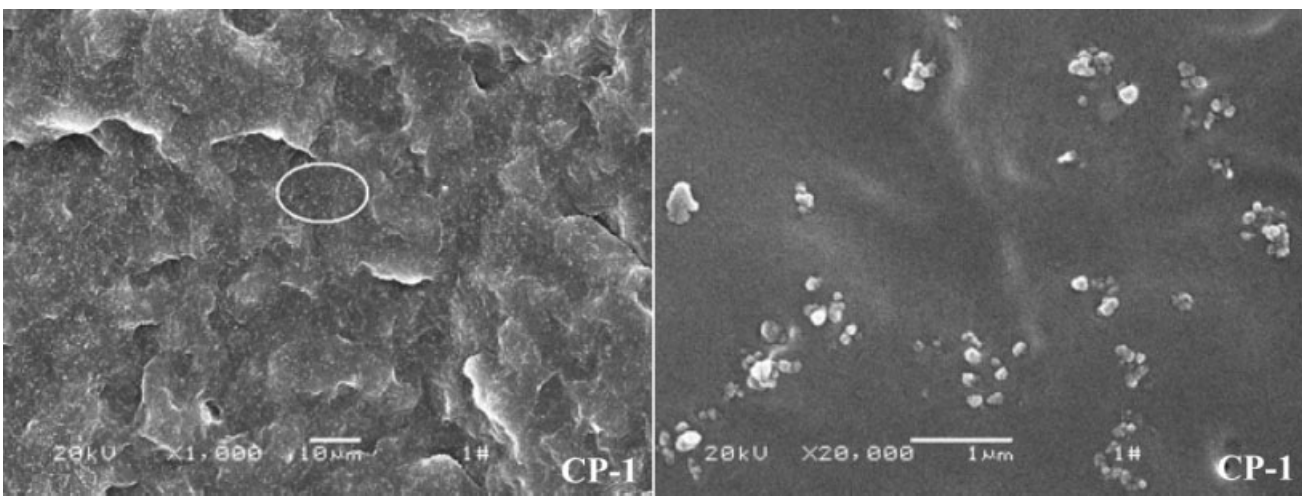


**Figure 1** SEM micrographs of the fractured surface of the CP-1 composite.

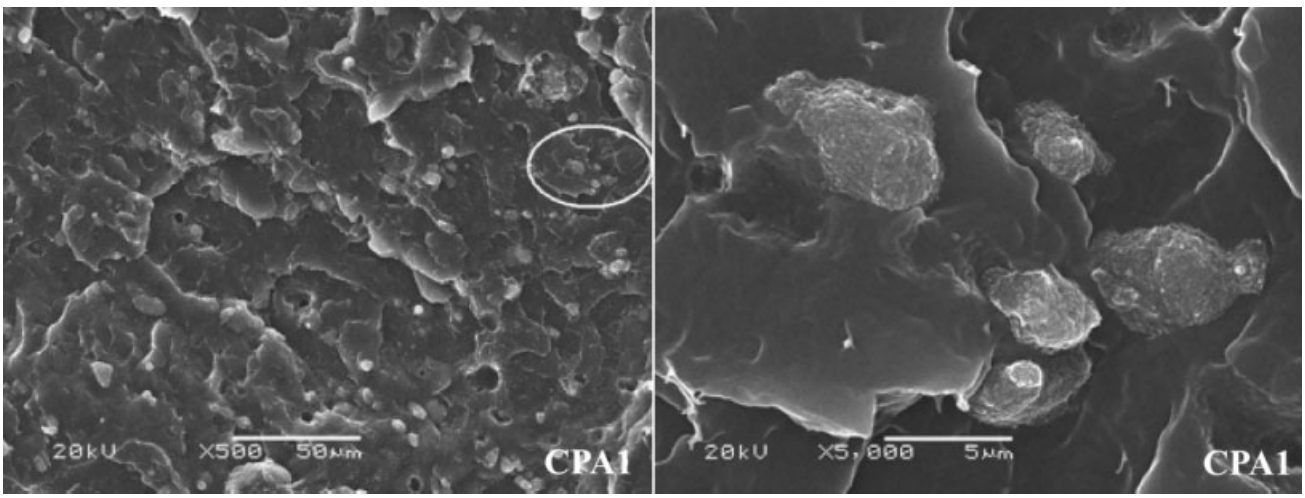


**Figure 2** SEM micrographs of the fractured surface of the CPA1 composite.

palladium alloy and examined by SEM (JSM-5900LV, JEOL, Tokyo, Japan) with an accelerating voltage of 20 kV. Some samples were pelletized to conduct differential scanning calorimetry (DSC; model 204, Netzsch, Bavaria, Germany).

## RESULTS AND DISCUSSION

From the interfacial tension values for PP/CB and PA6/CB, it was deduced that CB should be selectively dispersed in the PA6 phase in CB-filled PP/

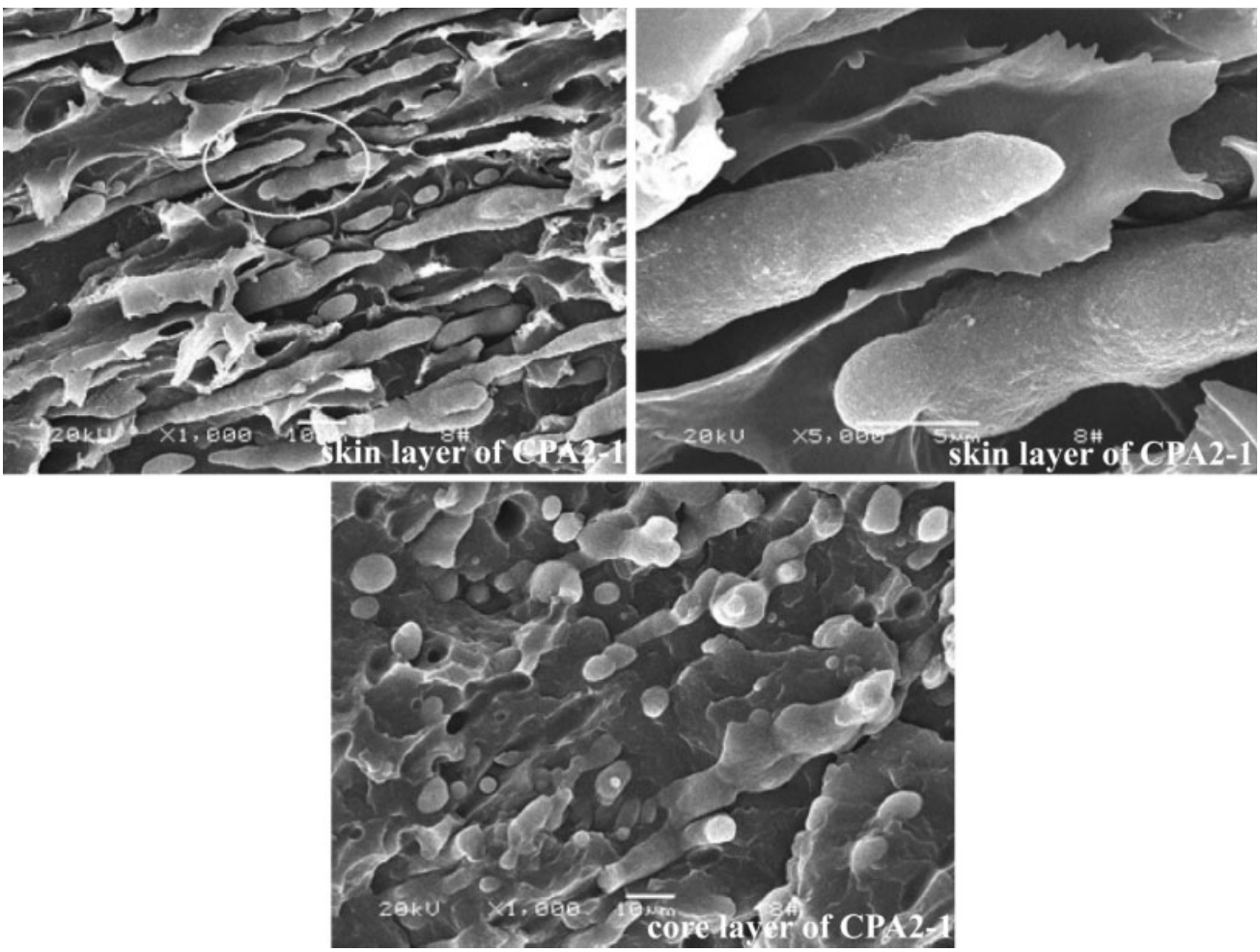


**Figure 3** SEM micrographs of the fractured surface of the CPA2-1 composite.

PA6 (CPA) composites. When $\varphi_{CB}$ in CPA is determined, the real $\varphi_{CB}$ value in the PA6 phase should be bigger enough to form a conductive network, and if the PA6 phase can be developed as a microfibrillar morphology, a more perfect conductive network should be obtained, and the electrical conductivity of CPA composites can be improved by the addition of PA6 to CP composites.

From Figures 1–5, we can conclude that there were typical multiphase structures for all kinds of CPA composites, with a continuous phase of PP and a dispersed phase of PA6. From them, it was determined that CB particles aggregated in the CP-1 composite, and in the CPA composites, almost all CB particles were dispersed in the PA6 phase; this indicated that the polar CB particles were selectively dispersed in the polar PA6 phase of these CPA composites.

When $\varphi_{CB}$ was kept fixed (2.5 vol %) as the PA6 content in these CPA composites was increased, there were obvious differences between their morphological structures. For CPA1, the weight ratio of PP to PA6 was 90/10, and the PA6 phase appeared as a sphere. For CPA2-1 and CPA3, the weight ratios of PP to PA6 were 80/20 and 70/30, respectively, and the PA6 phase appeared as microfibers. Meanwhile, the morphological structures of the skin layer and core layer of CPA2-1 and CPA3 were different; in CPA2-1, the microfibers of the core layer were much shorter than those of the skin layer, and in CPA3, the PA6 particles of the core layer almost appeared as spheres.

When $\varphi_{CB}$ was 5.0 vol % in CPA2-2, the dispersed particles appeared as spheres, and the morphological structure was similar to that of CPA1 (Figs. 2 and 5). However, apparently there were more and bigger dispersed particles in CPA2-2 than in CPA1; the volume resistivity decreased from $1.0 \times 10^{10}$ Ω cm for CPA1 to $2.2 \times 10^{2}$ Ω cm for CPA2-2 because of the connection of the dispersed particles in CPA2-2.

The content of the dispersed phase, the viscosity ratio of the dispersed phase to the matrix, the shear stress, and the cooling rate jointly determined the morphological structures for these composites. In our experiments, the shear stress and cooling rate were kept unchanged, so the content of the

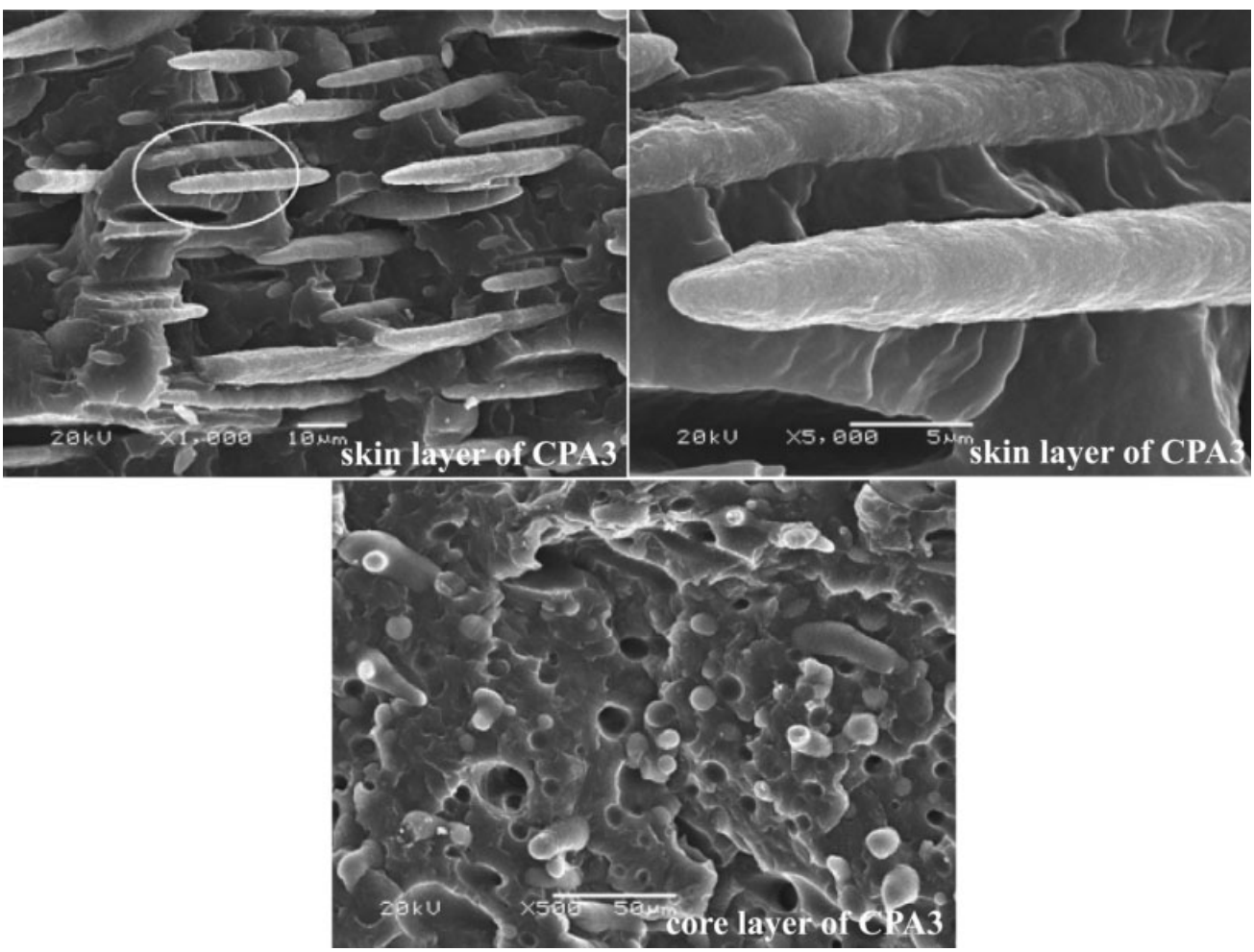


**Figure 4** SEM micrographs of the fractured surface of the CPA3 composite.

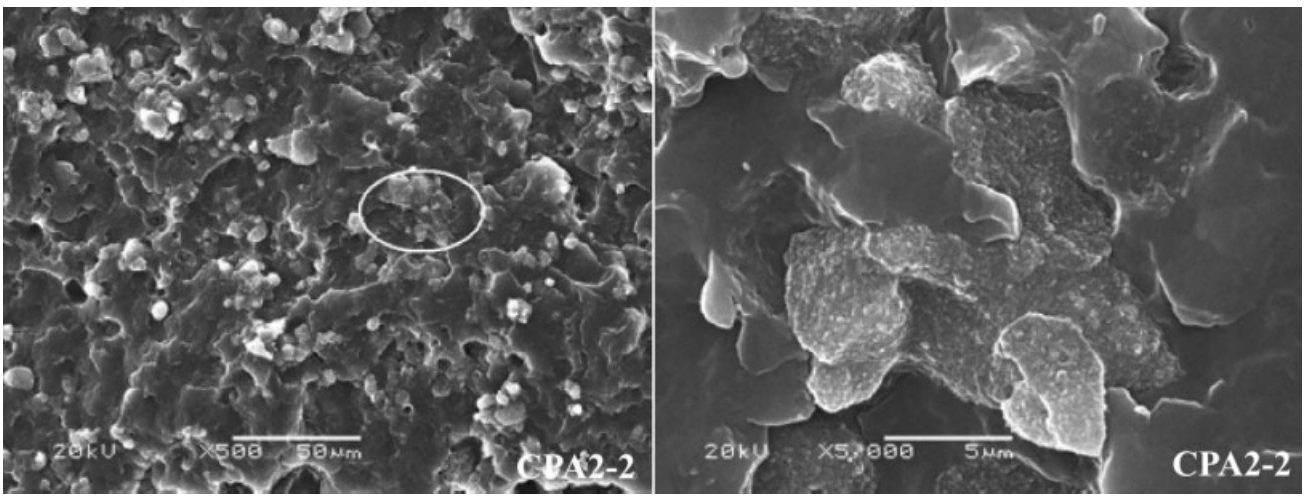


**Figure 5** SEM micrographs of the fractured surface of the CPA2-2 composite.

dispersed phase and the viscosity ratio of the dispersed phase to the matrix, that is, the contents of PA6 and CB, mainly affected the morphological structures of these composites. When the weight ratio of PP to PA6 was 90/10, the content of PA6 was not enough to form a continuous phase structure. For the composites of CPA2-1 and CPA3, the PA6 contents were high enough to form many dispersed particles that almost connected with one another. Meanwhile, when $\varphi_{CB}$ was kept the same (2.5 vol %) as PA6 in these CPA composites was increased, because of the selective dispersion of CB particles in the PA6 phase, the viscosity of the PA6 phase decreased; that is, the deformability of the PA6 phase increased, so the PA6 phase appeared as a sphere in CPA1 and as a microfibrillar structure in CPA2-1 and CPA3. In comparison with CPA3, $\varphi_{CB}$ in the PA6 phase of CPA2-1 was higher (Figs. 3 and 4), and this resulted in a higher viscosity for the PA6 phase and finally caused the morphological discrepancy between CPA2-1 and CPA3. $\varphi_{CB}$ in the PA6 phase and the morphological discrepancy determined a higher electrical conductivity for CPA2-1. During the molding process, the shear stress and cooling rate of the skin layer were higher than those of the core layer, so the microfibrillar structure of the skin layer was longer than that of the core layer and was kept down more perfectly. For CPA1 and CPA2-2, the deformability of the PA6 phases was the same because of a similar weight ratio of PA6 to CB, which resulted in similar morphological structures in these composites.

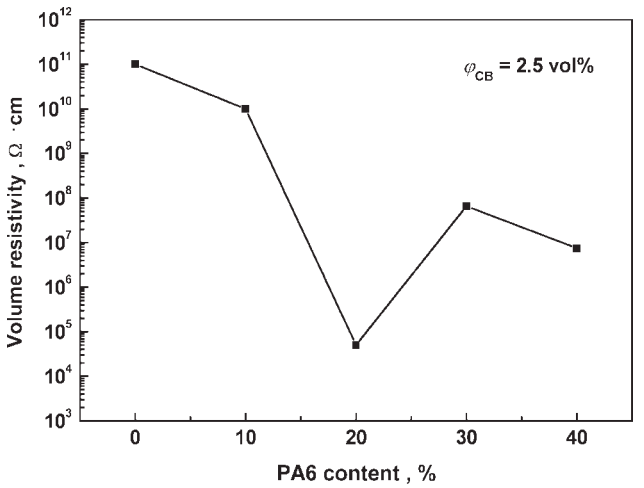


**Figure 6** Volume resistivity versus the PA6 content of CPA composites.

In brief, CB particles were selectively dispersed in the PA6 phase in CPA composites. When $\varphi_{CB}$ was 2.5 vol %, with an increase in the PA6 content in CPA composites, the microfibrillar structure of PA6 phase appeared, and for this structure, there was an optimal PA6 content in CPA composites. Apparently, the formation of microfibers facilitated the formation of an electrically conductive path, and this indicated that the volume resistivity of CPA composites decreased with an increase in the PA6 content and to a minimum at some PA6 content. Figure 6 shows that the introduction of PA6 into PP could remarkably decrease the volume resistivity of CP composites, and a minimum volume resistivity appeared when the weight ratio of PP to PA6 was 80/20. As shown in Table III, a comparison of CP

**TABLE III**
**Volume Resistivity of Different Systems**

| System | Volume resistivity ($\Omega \cdot$ cm) | System | Volume resistivity ($\Omega \cdot$ cm) |
|---|---|---|---|
| CP-1 | $1.0 \times 10^{11}$ | CP-2 | $3.0 \times 10^{6}$ |
| CPA1 | $1.0 \times 10^{10}$ | | |
| CPA2-1 | $5.0 \times 10^{4}$ | CPA2-2 | $2.2 \times 10^{2}$ |
| CPA3 | $6.6 \times 10^{7}$ | CPA4 | $7.4 \times 10^{6}$ |

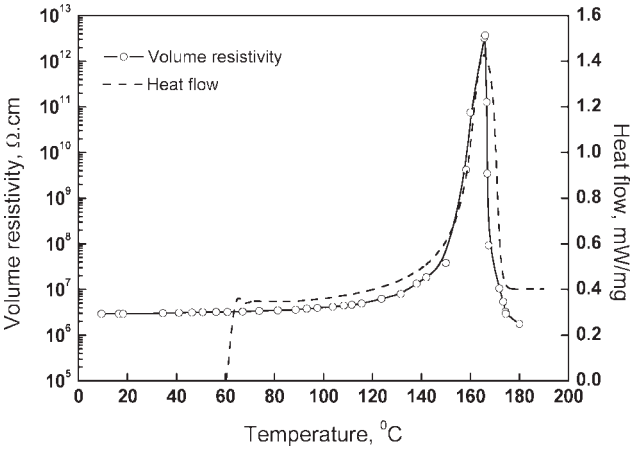


**Figure 7** Resistivity–temperature characteristics and DSC curve of the CP-2 composites.

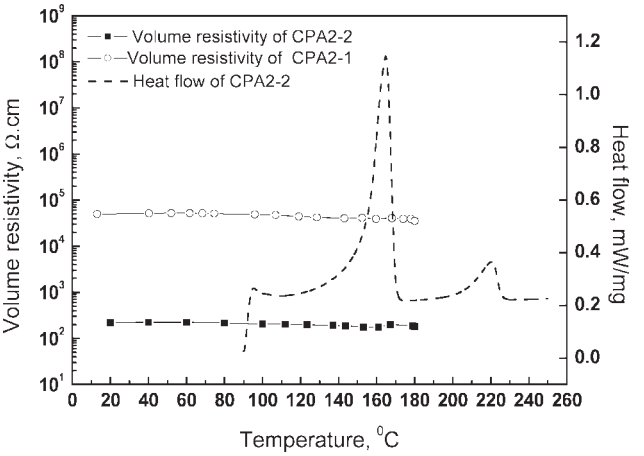


**Figure 9** Resistivity–temperature characteristics and DSC curve of the CPA2 composites.

composites with $\varphi_{CB} = 2.5$ vol % and $\varphi_{CB} = 5.0$ vol % reveals that the addition of PA6 could decrease the volume resistivity by 7 and 4 orders of magnitude, respectively.

Because of the selective dispersion of CB in the PA6 phase in CPA composites, from room temperature to the melting point of PP, PA6 remained almost unchanged in both its volume and its state of aggregation, and this could result in no PTC or negative temperature coefficient (NTC). The effects of PA6 on the resistivity–temperature behaviors of CP composites were studied.

Figure 7 shows the resistivity–temperature behavior and DSC curve of the CP-2 composite; there was an apparent PTC for the CP-2 composite in the melting range of PP followed by an apparent NTC, and the PTC and NTC intensities were about 6.1 and 6.3, respectively. [The PTC and NTC intensities are defined as $I_{PTC} = \log(\rho_{max}/\rho_i)$ and $I_{NTC} = \log(\rho_{max}/\rho_f)$, respectively, where $\rho_i$ is the initial electrical resistivity at room temperature (20°C), $\rho_{max}$ is the maximum electrical resistivity, and $\rho_f$ is the electrical resistivity at 180°C.] The CP-2 composite showed different resistivity–temperature behaviors during various thermal cycles (Fig. 8). The PTC and NTC intensities of the first heating were clearly bigger than those of the second heating and third heating, and the resistivity–temperature behavior of CP-2 showed an unrepeatable characteristic. When there was PA6 in the CPA2 composites (Fig. 9), the CPA2-1 and CPA2-2 composites showed different resistivity–temperature behaviors. The PTC and NTC disappeared even in the melting range of PP, and the resistivity of the CPA2-1 and CPA2-2 composites remained almost unchanged from room temperature to 180°C. Because of the big deformation of test samples, the resistivity of the CPA2-1 and CPA2-2 composites at temperatures higher than 180°C were not obtained. In addition, there were almost no effects of thermal cycles on the resistivity–temperature

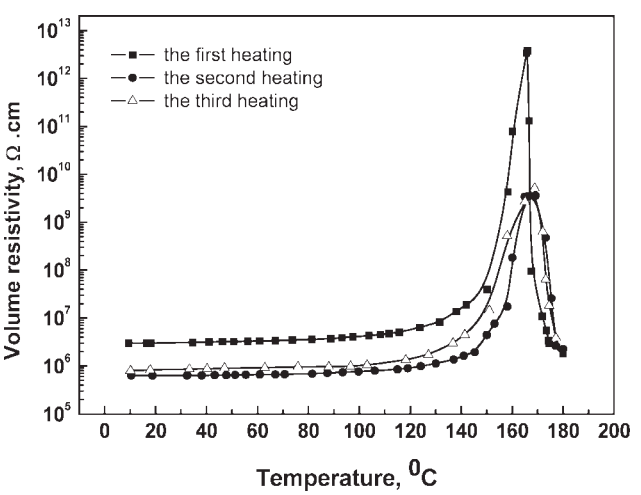


**Figure 8** Resistivity–temperature characteristics of the CP-2 composites during three heating cycles

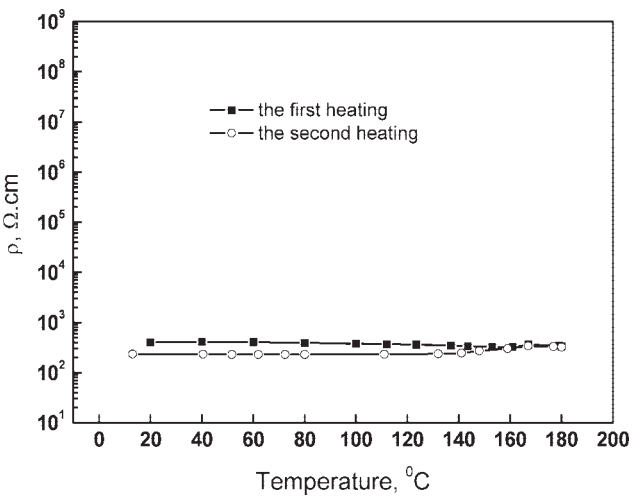


**Figure 10** Resistivity (ρ)–temperature characteristics of the CPA2-2 composite during two heating cycles.

behaviors of CPA2-2, and the resistivity–temperature behavior of CPA2-2 showed a repeatable characteristic (Fig. 10). In fact, it is well known that for PP, the transformation of the crystalline phase to the amorphous phase causes a significant volume expansion and a sudden increase in the resistivity due to the disconnection of the conductive paths; that is why there was an apparent PTC effect for the CP-2 composite in the melting range of PP. Generally, it is thought that the NTC effect is due to the redistribution of CB particles and CB–CB interaction.[21] When the temperature was in the melting range of PP, the restrained CB particles could be redistributed into a new amorphous area and connected to one another to set up new conductive paths, which resulted in a reduction of the resistivity of CP-2. Because of the redistribution of CB particles and CB–CB aggregation during the cooling process, an unrepeatable characteristic of resistivity for CP-2 appeared. For the CPA2-1 and CPA2-2 composites, when the CB particles were selectively dispersed in the PA6 phase and the composites were heated up to 180°C, the volume expansion effect of PP still appeared, but the volume expansion effect of PA6 remained small, and the redistribution of CB particles almost did not happen. The conductive networks remained unchanged, so there were no PTC or NTC effects from room temperature to 180°C, and the resistivity–temperature behavior of CPA2-2 showed a repeatable characteristic, verifying the selective dispersion of CB in the PA6 phase from another point of view. The slight difference in the resistivity–temperature behavior of CPA2-2 between the first and second heating cycles was due to the deformation and the change in contact resistance, which were caused by the first heating cycle.

## CONCLUSIONS

In all kinds of CPA composites, SEM results showed that CB particles were selectively dispersed in PA6 phases and rarely in PP phases. When the weight ratio of PP to PA6 was 90/10, PA6 particles appeared as spheres in the CPA1 composite. With an increase in the PA6 content, PA6 particles appeared as microfibers in the CPA2 and CPA3 composites, and this resulted in better conductive networks and a resistivity decrease of a maximum of 7 orders of magnitude in comparison with the CP composites. Because of the selective dispersion of CB in the PA6 phase, $\varphi_{CB}$ also affected the dispersed particle morphology. For the CB-filled PP composite, there were PTC and NTC effects with intensities of 6.1 and 6.3, respectively, in the melting range of PP, and an unrepeatable characteristic of resistivity appeared. However, for the CB-filled PP/PA6 composites, there were no PTC or NTC effects from room temperature to 180°C, and the resistivity–temperature behavior of CPA2-2 showed a repeatable characteristic, verifying the selective dispersion of CB in the PA6 phase. All the results indicate that an expected morphological structure can be realized and the electrical conductivity can be improved by the addition of PA6 to CP composites.

## References


1. Yoon, H. G.; Kwon, K. W.; Nagata, K.; Takahashi, K. Carbon 2004, 42, 1877.
2. Grunlan, J. C.; Gerberich, W. W.; Francis, L. F. J Appl Polym Sci 2001, 80, 692.
3. Hu, J.; Li, M.; Zhang, M.; Xiao, D.; Cheng, G.; Rong, M. Macromol Rapid Commun 2003, 24, 889.
4. Tjong, S. C.; Liang, G. D.; Bao, S. P. Scr Mater 2007, 57, 461.
5. Hu, G.; Zhao, C.; Zhang, S.; Yang, M.; Wang, Z. Polymer 2006, 47, 480.
6. Garmabi, H.; Naficy, S. J Appl Polym Sci 2007, 106, 3461.
7. Nogales, A.; Broza, G.; Roslaniec, Z.; Schulte, K.; Sics, I.; Hsiao, B. S.; Sanz, A.; Garcia-Gutierrez, M. C.; Rueda, D. R.; Domingo, C.; Ezquerra, T. A. Macromolecules 2004, 37, 7669.
8. Zou, J.; Yu, Z.; Pan, Y.; Fang, X.; Ou, T. J Polym Sci Part B: Polym Phys 2002, 40, 954.
9. Lu, W.; Lin, H.; Wu, D.; Chen, G. Polymer 2006, 47, 4440.
10. Hao, X.; Gai, G.; Yang, Y.; Zhang, Y.; Nan, C. Mater Chem Phys 2008, 109, 15.
11. Dang, Z.; Wu, J.; Xu, H.; Yao, S.; Jiang, M. Appl Phys Lett 2007, 91, 072912.
12. Gelves, G. A.; Lin, B.; Sundarara, U.; Haber, J. A. Adv Funct Mater 2006, 16, 2423.
13. Sandler, J. K. W.; Kirk, J. E.; Kinloch, I. A.; Shaffer, M. S. P.; Windle, A. H. Polymer 2003, 44, 5893.
14. Al-Saleh, M. H.; Sundararaj, U. Compos A 2008, 39, 284.
15. Baker, W.; Scott, C.; Hu, G.-H. Reactive Polymer Blending; Hanser: Munich, 2001; p 120.
16. Sundararajs, U.; Macosko, C. W. Macromolecules 1996, 28, 2647.
17. Ghodgaonkar, P. G.; Sundararaj, U. Polym Eng Sci 1996, 36, 1656.
18. Masao, S.; Kazuya, S.; Shigeo, A.; Keizo, M.; Hideaki, N. Polym Bull (Berlin) 1991, 25, 265.
19. Wu, G.; Asai, S.; Sumita, M. Macromolecules 2002, 35, 945.
20. González-Martín, M. L.; Jańczuk, B.; Labajos-Broncano, L.; Bruque, J. M. Langmuir 1997, 13, 5991.
21. Tang, H.; Chen, X.; Luo, Y. Eur Polym J 1997, 33, 1383.